ACS APPLIED MATERIALS & INTERFACES

www.acsami.org

Research Article

Hyper-Cross-Linked Polymer-Decorated Surfaces with Ultrahigh Efficiency for Oil/Water Emulsion Separation and Recovery

Qi Sheng, Wendy Tian,* and Colin D. Wood*

Cite This: *ACS Appl. Mater. Interfaces* 2021, 13, 39925−39933

Read Online

ACCESS | Metrics & More | Article Recommendations | Supporting Information

ABSTRACT: A novel superhydrophobic/superoleophilic surface has been developed by direct surface condensation of dichloroxylene that results in a controlled coating of hyper-cross-linked polymers. Specifically, the coating was successfully applied to a melamine formaldehyde sponge and optimized by fine-tuning the reaction variables. The resulting hierarchical porous sorbents stabilized by polydimethylsiloxane exhibited an increased surface area, good physiochemical stability, high selectivity, and adsorption capacities for a variety of oils and solvents. The composite can separate oil in water emulsions with ultrahigh separation efficiency >99% over 10 cycles in liter-scale experiments, wherein the highest separation efficiency was as low as 2 ppm even with a short period of filtration, suggesting strong potential for oil/water separation and recovery.

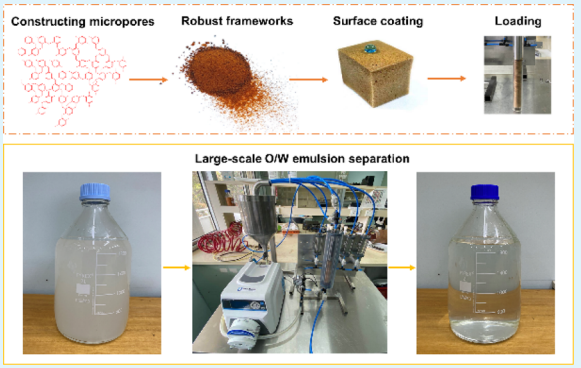

KEYWORDS: *hyper-cross-linked polymers, polydimethylsiloxane, hierarchical structures, superhydrophobic, superoleophilic, emulsion separation*

1. INTRODUCTION

Oil spill incidents have an adverse impact to the marine ecosystem, economy, and society all over the world.[1−3] To minimize these consequences, an appropriate material for oil spill cleanup and recovery is required. This presents a number of technical challenges requiring the surface to be optimized in terms of chemistry, surface area, charge, roughness, and environmental profile. Ideal materials possess superhydrophobicity, high porosity, surface area, and selectivity to hydrocarbons. In addition, the pore size of any material must be tailored to allow rapid uptake while avoiding clogging and maintaining high uptake particularly under representative conditions that would be encountered during a spill. Any material must also be recyclable and easy to operate under conditions encountered during an oil spill response. In addition, the materials must be inexpensive and scalable. All these factors mean that progress in this field has been challenging. One approach that has been explored is using nanotechnology for improved separation and recovery during the oil spill response, which has been reported to have encouraging outcomes.[3] This includes meticulously engineered porous fabrics/fibers,[4,5] sponges/foams,[6−8] metal meshes,[9−11] membranes,[12,13] ceramics,[14] aerogels,[15,16] free-standing porous materials[17,18] with superwetting properties, which are typically superhydrophobic/superoleophilic and superhydrophilic/superoleophobic (in air or under water), and responsive moieties. However, many are limited to a laboratory scale with disadvantages such as expensive starting materials, complicated synthesis procedures, lack of durability, low flux, fouling, challenging regeneration, and long-term operation. This study presents a robust hierarchical porous superhydrophobic sponge achieved by nanocoating of hyper-cross-linked polymers (HCPs) that have the potential to overcome some of these issues.

HCPs are an important class of permanently microporous materials that have promise for a broad range of applications such as gas storage, carbon dioxide capture, water treatment, drug delivery, separation, catalysis, and sensing.[19−21] They have been extensively studied in the past few decades owing to many distinct advantages such as diverse synthetic routes, low-cost reagents, mild reaction conditions, ease of functionalization, and high surface area. Nevertheless, existing studies are more focused on fundamental examination from a gas sorption perspective and synthetic routes rather than applications of HCPs.[19] While some commercial HCP sorbents have already been used as highly effective alternatives to activated carbon for organic and metal ion removal in wastewater treatment,[22] there is limited research on the application of HCPs for oil spill cleanup. We envisioned that HCPs are also capable of

Received: June 17, 2021
Accepted: August 3, 2021
Published: August 12, 2021

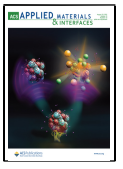

https://doi.org/10.1021/acsami.1c11302
ACS Appl. Mater. Interfaces 2021, 13, 39925−39933

separating hydrocarbons from water in the field of oil spill response as demonstrated in our earlier study via hyper-cross-linking of a polymerized high internal phase emulsion (PHIPE). In particular, we investigated a three-dimensional (3D) hierarchically porous HCP monolith comprising abundant macropores and nanopores of a high surface area of 196−595 m^2 g^{-1} with an oil adsorption capacity of 800−1900% of its own weight, suggesting the potential application of HCPs for an oil spill response.[18] However, the fabrication of such materials involves polymerizing HIPEs, which presents challenges in terms of large-scale applications. To the best of our knowledge, we report for the first time an HCP-decorated hierarchically porous sorbent where porous HCPs were introduced to the macroporous substrate for oil/water separation. Notably, this strategy is potentially a universal method for all desired surfaces, and the facile fabrication is inexpensive, affordable, and simple to scale-up.

Melamine formaldehyde (MF) sponges were selected as the ideal substrate in this study because the 3D interconnected framework gives rise to high permeability for oil adsorption and its intrinsic flexible skeleton makes the material mechanically robust.[23,24] There have been some studies reporting microporous material-coated sponges,[25−29] but these do not include HCPs. Jiang et al. developed a hydrophobic metal organic framework (MOF)-coated sponge incorporated with $-CF_3$ fluorine groups, overcoming the vulnerability that most MOF materials have in the presence of water/moisture. The coated sponge takes up 1200−4300% of organic pollutants including oils and can be used for continuous oil spill cleanup assisted with a self-priming pump.[27] Xu et al. made a hydrophobic MOF-coated sponge with an excellent oil adsorption capacity ranging from 6600 to 13,000%.[29] Sun et al. successfully imparted superhydrophobicity on the sponge via the coating of covalent organic frameworks (COFs) postmodified with 1*H*,1*H*,2*H*,2*H*-perfluorodecanethiol. The composite exhibited remarkable sorption capacities from 6700 to 14,200%.[28] MOFs and COFs are another class of microporous material similar to HCPs, but they are crystalline unlike the amorphous HCPs. They offer great promise across a number of fields, but challenges lie in the complex synthesis conditions and scale-up of inexpensive stable structures.[25,26] Compared with these emerging microporous materials, HCPs have advantages in terms of inherent stability, efficient fabrication, and comparable functions through surface coating. Nevertheless, none of the aforementioned microporous material-coated sponges were reported to demonstrate the feasibility of oil/water emulsion separation, which is a much more serious challenge to any new material.

In this work, we demonstrate the controlled coating of nanosized HCPs on a sponge to transition the wettability from hydrophilicity to superhydrophobicity. The material was fabricated using a direct surface coating of low-cost and mild operating conditions, which offers advantages in terms of easier scale-up. The novel sorbent in conjunction with a silicone elastomer formed a robust porous surface,[30−32] which has an addition of specific surface area, good mechanical, chemical, and thermal stability, high selectivity, and adsorption capacities over various oils and organic solvents. The oil in water emulsion (O/W) separation performance was evaluated through large-scale apparatus for carrying out liter-scale tests, which confirmed the ultrahigh efficiency of HCP-coated sponges as a sorbent filter for practical application such as tertiary treatment.

2. EXPERIMENTAL SECTION

2.1. Materials. Commercial melamine sponges were purchased from commercial sources but were manufactured by BASF. *p*-Dichloroxylene (DCX) was purchased from Alfa Aesar; iron(III) chloride (anhydrous $FeCl_3$, 97%), Sylgard 184 (polydimethylsiloxane), kerosene, and hexane (95%) were purchased from Sigma-Aldrich; 1,2-dichloroethane (DCE, 99.8%), diethyl ether (99.7%, RCI Labscan), ethanol (99.5%), acetone (99.5%), and silicone fluid (350 cSt) were purchased from Chem-Supply; methanol (99.8%), tetrahydrofuran (99.9%), toluene (99.9%), and chloroform (99.8%) were purchased from Merk; Tellus S2 M 32 was obtained from Shell & Turcas Petrol AS; and conventional heavy crude oil was obtained from the department of Fisheries and Oceans Canada.

2.2. Preparation of MF-HCP. A piece of melamine sponge was cleaned with ethanol and water for 30 min in an ultrasonic bath and dried at 100 °C for 24 h. The as-prepared sponge was immersed in a solution of dichloro-*p*-xylene that was dissolved in anhydrous DCE and stirred for 5 min. Another solution of $FeCl_3$ was then added to initiate the Friedel−Crafts reaction. The resulting mixture (0.25%/3.125 mg mL^{-1}) was stirred at 100 rpm at room temperature for 20 h. The HCP-coated sponge denoted as MF-HCP was then taken out from the mixture and washed with water, methanol, and diethyl ether followed by drying overnight at 80 °C.

2.3. Preparation of MF-HCP-PDMS. The MF-HCP was immersed in a mixture of PDMS and a curing agent at a weight ratio of 10:1 in toluene for 15 min followed by curing at 120 °C for 20 h. To compare the influence of PDMS coating upon the HCP-decorated sponge, samples with different concentrations of PDMS 0.5, 1, 2, and 3% were prepared and denoted as MF-HCP-PDMS-0.5, MF-HCP-PDMS-1, MF-HCP-PDMS-2, and MF-HCP-PDMS-3, respectively.

2.4. Characterization of Hyper-Cross-Linked Polymer-Coated Sponges. The surface morphology was investigated by scanning electron microscopy (SEM), and its surface chemical composition was revealed by elemental analysis. In detail, the samples were mounted on an aluminum stub with a double-sided conductive carbon tape; then, iridium was coated using a Cressington 208HRD sputter coater to an approximate thickness of 4 nm. The samples were imaged using a Zeiss Merlin FESEM (field-emission scanning electron microscope) operated in the secondary electron (SE) mode. Energy-dispersive spectroscopy (EDS) was used to identify elements present using an AZTEC system by Oxford Instruments Pty Ltd. using an X-Max Extreme 100 mm^2 windowless Silicon Drift Detector (SDD). An accelerating voltage of 3 kV was used for imaging and EDS analysis. The results are to be taken as semiquantitative and only trends are compared. Scale bars are shown in the images indicative of the magnifications used. The static water contact angle was measured using First Ten Ångstroms 1000 using 10 μL droplets and an average of three measurements were taken. The specific surface area was determined by Brunauer−Emmett−Teller (BET) analysis. Specifically, nitrogen gas adsorption isotherms at a pressure in the range of 0−1.2 bar were measured by a volumetric method using a Micromeritics 3Flex instrument. Freshly prepared samples were transferred to a predried and weighed analysis tube, which was stoppered with a Transeal cap. The sample was evacuated and activated at 100° C under dynamic vacuum at 10−6 Torr for 24 h. Accurate sample masses were calculated using degassed samples. Ultrahigh purity N_2 gas was used for the experiments. N_2 adsorption and desorption measurements were conducted at 77 K. Surface area measurements were performed on N_2 isotherms at 77 K using the BET model with adsorption values increasing in the range from 0.05 to 0.2 relative pressure. The size distribution of micro-nano oil in water emulsions was determined by Zetasizer Nano ZS by three repeating experiments.

2.5. Oil Adsorption Experiment. The adsorption capacities of HCP sponges were measured by immersing the samples into organic

https://doi.org/10.1021/acsami.1c11302
ACS Appl. Mater. Interfaces 2021, 13, 39925−39933

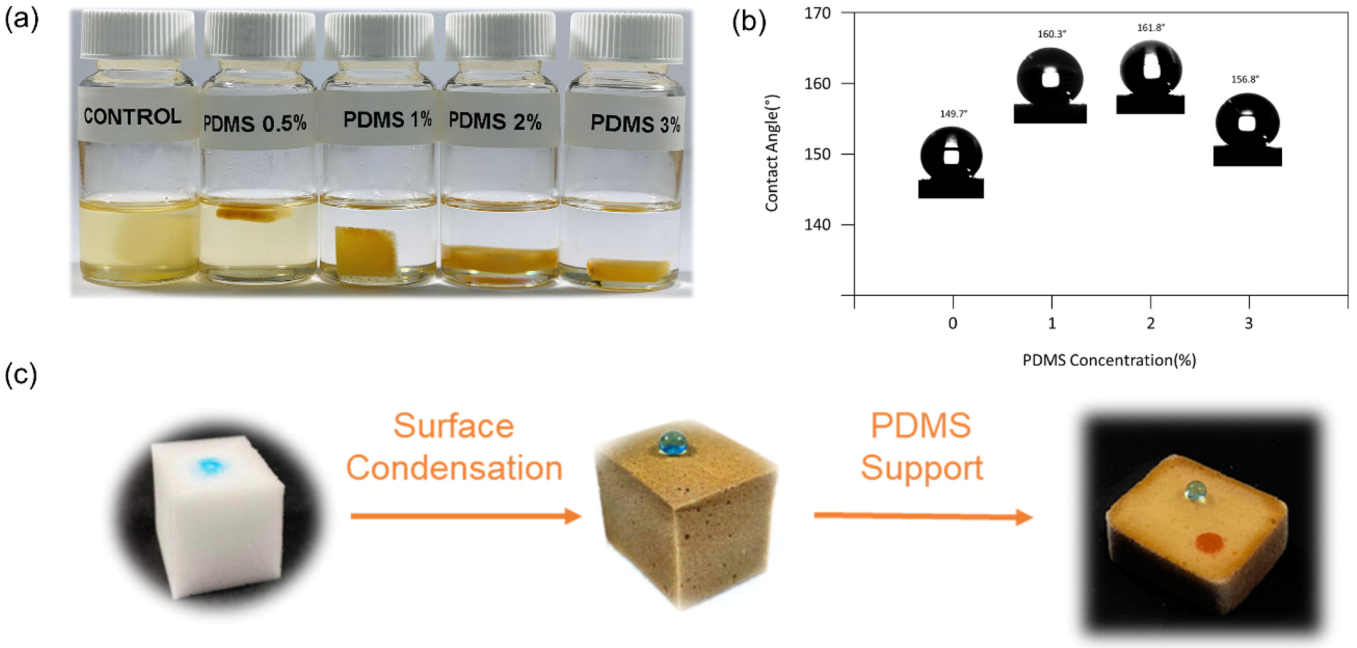

Figure 1. (a) Coating stability against mechanical forces examined by ultrasonicating the samples in toluene for 15 min. The MF-HCP as the control and MF-HCP-PDMS sponges generated at different PDMS concentrations 0.5, 1, 2, and 3% were labeled, respectively. (b) Contact angle of sponges as a function of PDMS concentrations. (c) Fabrication of MF-HCP-PDMS (the deionized water dyed with methylene blue was used to show the wettability transition of the pristine sponge from hydrophilicity to superhydrophobicity as a result of the HCP coating, and toluene dyed with Sudan red was used to demonstrate the superoleophilicity of the composite).

solvents and oils until saturated and then the samples were weighed immediately to avoid the evaporation of sorbates. Each experiment was performed in triplicate to obtain average values, which were calculated by the equation: adsorption capacity $(k) = (m_a - m_o)/m_o$, where m_o and m_a represent the mass of the sample before and after the oil adsorption experiments. For regeneration, adsorption and desorption of the model oil (Shell Tellus S2 M32) by sponges were repeatedly performed in each cycle. The dried samples were soaked in the oil and weighted initially. Then, the saturated samples were loaded in tubes separately and centrifuged for 5 min at 4000 rpm at room temperature followed by another weighing.

2.6. O/W Emulsion Preparation. The oil in water emulsion was prepared using a homogenizer HG-15A purchased from DAIHAN Scientific. O/W emulsion (1000 ppm) was used, as the aim of the study is to prove the promise of HCP sponge for diverse applications such as tertiary treatment technologies for decanting during an oil spill response. In detail, the mixture of 2000 mg model oil and 1998 mL deionized water was prepared and homogenized at 6000 rpm until a stable emulsion was formed.

2.7. O/W Emulsion Separation. To investigate the O/W emulsion separation performance, a liter-scale separator was fabricated. This apparatus comprised filter media holders, reservoir tank, pressure monitor, air compressor, and vacuum pump mounted on a platform. Therein, 2 g of MF-HCP-PDMS was loaded as the filter in a stainless-steel cylinder, where 2 L of 1000 ppm O/W emulsion in the reservoir tank was pumped through for the performance test. The certain flow rate and separation time were applied and total petroleum hydrocarbon (TPH) of the filtrate was analyzed by a local commercial analytical company Leeder Analytical, which is specialized at hydrocarbon fingerprinting. For sorbent regeneration, a solvent washing method was found efficient with an air blowing feature for rapid drying after oil extraction.

3. RESULTS AND DISCUSSION

3.1. Synthesis of the Superhydrophobic HCP-Decorated Sponge. The major advantages of HCPs for an oil spill response are the molecular structure, rigid network, permanent porosity, and high surface area. However, the poor solution processability of HCPs has limited their versatility for many applications. Unlike polymers of intrinsic microporosity (PIMs), HCPs are insoluble in solvents and are difficult to process into devices for many industrial uses while handling in particle form is not desirable.[33,34] It is also challenging to use preformed HCPs from bulk synthesis as a coating material due to the nature of the Friedel–Crafts reaction that proceeds rapidly and randomly even under ambient condition and often generates polydisperse particles in the micron size range (Figure S1). The appropriate particles for coating upon a desired surface, however, should have a controlled size, which would lead to homogenous distribution and stable attachment.

In this study, we have coated nanosized HCPs upon a substrate via direct surface condensation of dichloroxylene (DCX). This was achieved by manipulating all possible variables including building blocks (starting monomers), external cross-linkers, as well as concentration, time, pressure, and temperature of the reaction, which could determine the final coating characteristics. Ambient conditions were chosen for this reaction out of practical scale-up purpose. Concentration and time of the reaction were fine-tuned to control the film density (loading) and degree of cross-linking of the HCPs on the commercial melamine sponge. Therein, the degree of cross-linking is crucial to the resultant particle size and surface area of the polymers.

A series of concentrations by mass, that is, 0.1, 0.25, 0.5, 1, and 2% of DCX dissolved in DCE, has been used for surface coating, respectively (Figure S2a). It was found that the higher the concentration, the faster the reaction proceeded, resulting in a higher degree of cross-linking as well as the amount of particle loading. The 1 and 2% reaction mixtures began the surface condensation reaction at the mixing of DCX and $FeCl_3$ solutions in the presence of the sponge and caused too many

https://doi.org/10.1021/acsami.1c11302
ACS Appl. Mater. Interfaces 2021, 13, 39925−39933

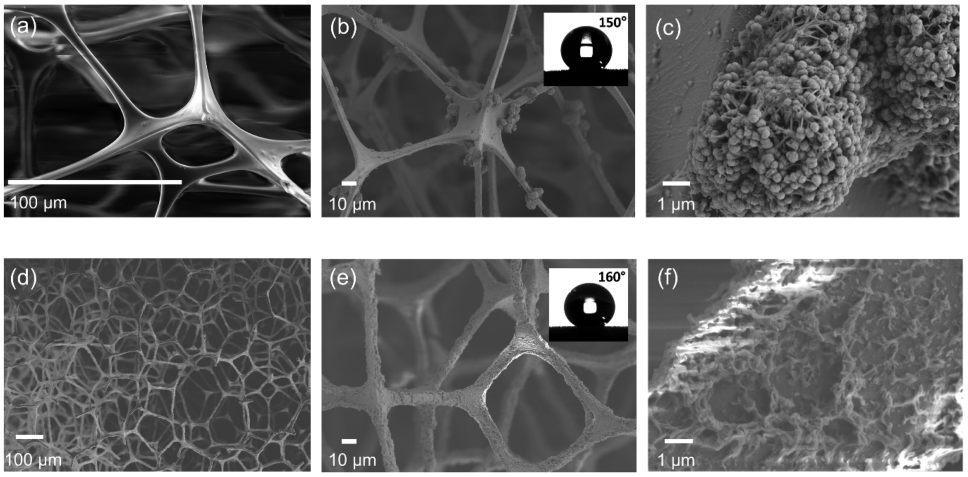

Figure 2. SEM images of (a) pristine melamine foam; (b, c) MF-HCP at a magnification of 500× and 1000×; (d–f) MF-HCP-PDMS-1 at a magnification of 100×, 500×, and 1000×.

HCP particles to quickly form, while the reaction rate of 0.1% was drastically retarded due to the lowest concentration, and the coating could not be visually observed on the sponge. Correspondingly, the appearance of the decorated surface varied from dark brown to pale yellow reflecting the different cross-linking degrees and loadings of HCPs. Further scale-up experiments at 0.25% with a prolonged reaction time of 20 h was found to provide the most preferable coating, in terms of particles distribution on the surface (Figure S2b). In comparison, the coating resulting from 0.5% solution was incomplete with the center of the sponge visually showing no coating, which was possibly due to the detachment of larger particles from the surface during the reaction (Figure S2c). The increased reaction time contributed to a higher cross-linking degree of HCPs for coating application at a given concentration. The uniformly coated sponge MF-HCP 0.25% had mass increase about 69%, which indicated sufficient loading for applications. However, it was found that the resulting composite was susceptive to mechanical loss of the HCPs. Therefore, PDMS was utilized to fix the HCP because it is known for its durable and elastic properties and has been widely used to bridge the nanoparticles to the surface. Hence, thermally curable PDMS of different concentrations was further applied to improve the stability of the HCP coatings. As seen in Figure 1a HCP coating without PDMS can shed off completely in an ultrasonic bath within 15 min. By comparison, sponges coated with PDMS at concentrations over 1% can survive the same harsh test as well as other external forces such as extrusion and shredding and no obvious particle loss can be observed. Moreover, the use of PDMS resulted in a considerable increase in the water contact angle varying with the concentrations, as shown in Figure 1b, which is favorable for oil/water separation application. The scheme of the fabrication of the robust superhydrophobic HCP sponge is shown in Figure 1c.

3.2. Surface Morphology. To confirm that a homogeneous coating was generated, SEM was utilized to observe the microstructural and surface morphology of the sponge without coating and compared to the HCP-decorated sponge. As shown in Figure 2a, the pristine sponge has an open, interconnected network of a smooth skeleton with pore sizes around 150 μm, showing large macropores and volume. As shown in Figure 2b, the sponge retains its inherent structure, pore size, and porosity after coating with HCPs. The nanoparticles deposited on the skeleton homogeneously, resulting in an obvious change of surface morphology. A thin base film of polymers formed throughout the sponge, altering the original appearance and roughness of the sponge. Moreover, emerging small bulges and large clumps further contributed to the establishment of the hierarchical architecture (Figure S3). Larger clumps may develop from small bulges as a result of smaller nanosized HCPs that assembled and cross-linked. This is also confirmed by Fourier transform infrared (FTIR) spectroscopy results (Figure S4) with the emerging band around 2921 cm^{-1} indicating the presence of HCP containing C–H bonds. The morphology looked interestingly like a cluster where the network of the submicron spheres with a diameter 300–500 nm was supported by numerous "trunks" (Figure 2c). Figure 2d–f shows a significant morphology change after the incorporation of PDMS top layers; the macroporosity of the sponge remained the same with a slightly reduced pore diameter about 140 μm, while the overall roughness was further enhanced, and the majority of HCP particles were sparingly covered with PDMS, forming a new intertwined porous networks; this was in good agreement with Figure S4 where the strong bands of Si–O–Si and $Si-CH_3$ appeared at 789, 1010, and 1258 cm^{-1}, respectively. In general, SEM imaging of this complicated micro-nano hierarchical structure consisting of a base film, small bulges, large clumps, and a PDMS top layer has showed that this novel porous coating has been successfully generated upon the sponge.

3.3. Surface Area. HCPs typically have high surface area when synthesized in the bulk phase due to the high degree of cross-linking in the network in the solvent swollen state, which prevents collapse of the structure on drying. We envision that the presence of HCP nanoparticles on the sponge should provide an extra surface area despite the limited cross-linking degree due to the low reaction concentration for optimal coating. To verify the hypothesis, the total surface areas of MF-HCP, $HCP_{surface}$, and HCP_{batch} have been investigated as part of coating characteristics. The BET analysis shown in Table S1 confirms this. It is worth noting that the BET surface area of the pristine sponge is not applicable because the macroporosity goes beyond the multilayer gas sorption theory. In contrast, the surface area of the coated sponge was 41.1 $m^2\ g^{-1}$, indicating

https://doi.org/10.1021/acsami.1c11302
ACS Appl. Mater. Interfaces 2021, 13, 39925–39933

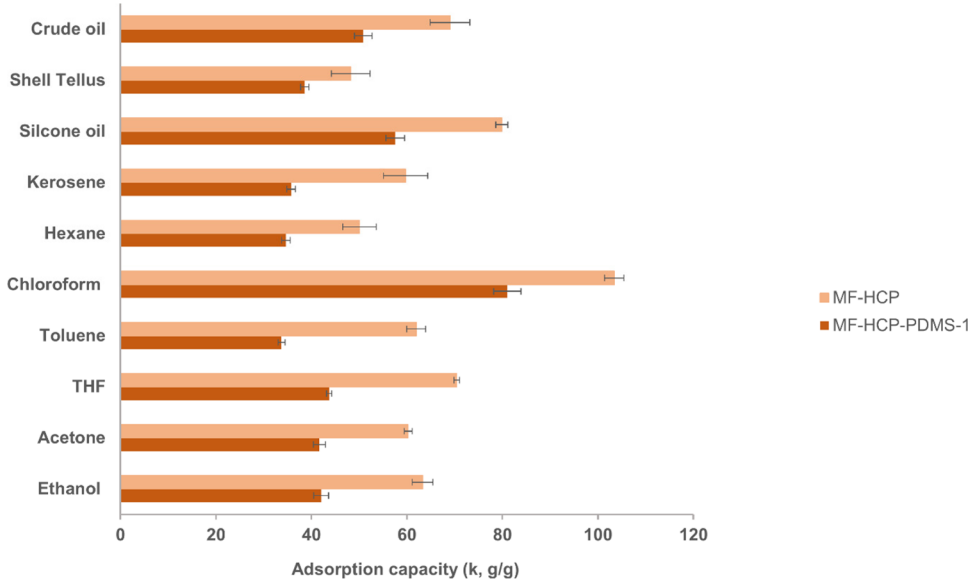

Figure 3. Adsorption capacities of MF-HCP and MF-HCP-PDMS-1 toward a variety of solvents and oils.

the successful incorporation of nanoporous materials. The surface area of an HCP synthesized in bulk is typically >1000 $m^2\ g^{-1}$, but the overall amount of HCP on the foam is limited, so the increase in surface area from essentially zero for the pristine foam to 41.1 $m^2\ g^{-1}$ is a strong indication of the porous structure of the HCP. $HCP_{surface}$ has a similar average pore size to MF-HCP, while the surface area and pore volume are twofold more than that of MF-HCP, suggesting that the surface area and pore volume of MF-HCP are inversely proportional to the weight of the composite on the grounds that MF-HCP consisted of 41% nanoparticles and 59% sponge calculated by weighing before and after. The surface area of $HCP_{surface}$, however, is not comparable with that of HCP_{batch}, which is in good agreement with the previous discussion that the reaction concentration has a major influence on the degree of cross-linking and thus the resultant particle size and surface area of the HCPs (Figure S5). To further investigate the influence of PDMS outermost coating on MF-HCP, the surface areas of MF-HCP-PDMS-1, MF-HCP-PDMS-2, and MF-HCP-PDMS-3 were measured. The BET results revealed that MF-HCP with 1% PDMS almost maintained its original surface area whereas 2 and 3% PDMS greatly reduced the surface area because the excess amount of PDMS began to block the pores of HCPs. In all cases, PDMS coating reduced the pore volume and pore size. Also, a slight decrease in the water contact angle with 3% PDMS (Figure 1b) can be seen, suggesting a counteraction effect upon the surface roughness. In summary, though at the expense of compromised surface area, the regulated nanosized particles are advantageous for coating application over HCPs from bulk synthesis and the loading amount is appropriate for the desired surface. Furthermore, MF-HCP-PDMS-1 was determined to be the preferable candidate in terms of surface area, robustness, and superhydrophobicity, which were essential for oil/water emulsion separation.

3.4. Superwettability, Adsorption Capacity, and Recyclability. The surface morphology and chemistry are known to determine the surface wettability that are closely related to oil adsorption. The hydrophobicity enhances the adsorption of oils simultaneously preventing the uptake of water. Therefore, superhydrophobic sorbents with high selectivity are one of the most promising designing strategies. The nanocoating of HCPs reported in this study can transform the hydrophilic melamine sponge to superhydrophobic surface with a water contact angle of about 150° in one step (Figure 1c and Figure 2b). This is attributed to the inherent physicochemical properties of HCPs, including the hydrophobicity from low surface energy of repeating benzene units and hierarchical roughness by the hyper-cross-linked porous framework disturbed on the surface altered the wetting properties drastically. In addition to the superhydrophobicity, the superoleophilic feature of the HCP-decorated surface was found outperform the hydrophobic surface coated with PDMS only as a control. Figure S6 shows that both MF-HCP-PDMS and MF-PDMS have an oil contact angle of 0°, but the time-lapse images reveal the exceeding adsorption rate of MF-HCP-PDMS compared to MF-PDMS. The modified sponge repels water even by pressing down into the water and shows a "silver mirror" effect (Movie S1). This phenomenon is caused by the reflection from the thin layer of air trapped in the hierarchical architecture, which is a signature of the Cassie state.[35] The composite bounces off the water around itself and floats on the top immediately when the pressure is released, leaving the surface unwetted. When in the scenario of floating oil on the water surface or heavy oil under water, this vast volume composite with superoleophilic character can readily transport the hydrocarbons from water into the hierarchical pores at the contact of the oils and solvents though capillary effects (Movies S2 and S3).

To further investigate the superwettability of HCP-decorated sorbents, a range of organic solvents and oils were used for adsorption experiment (Figure 3). Depending on the different polarities, viscosities, and densities of sorbates, MF-HCP exhibits superior adsorption capacities ranging from 4800 to 10,300%, while MF-HCP-PDMS-1 showed lower capacities 3400−8100%. This can be owed to the mass increase of PDMS coating, which in turn decreases the adsorption capacities calculated by adsorption of sorbates dividing mass in total. This trend can be confirmed by further increasing the concentration of PDMS coating (Figure S7). The regeneration

https://doi.org/10.1021/acsami.1c11302
ACS Appl. Mater. Interfaces 2021, 13, 39925−39933

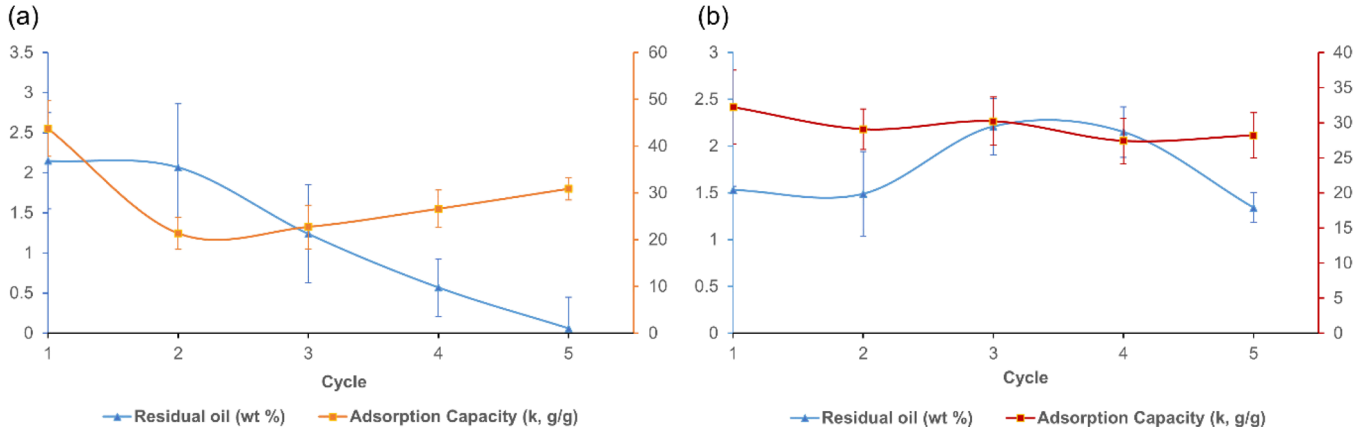

Figure 4. Recyclability of (a) MF-HCP and (b) MF-HCP-PDMS-1 over Shell Tellus oil.

Scheme 1. Configuration of the O/W Emulsion Separator and Separation Mechanism of the HCP Sorbent Filter

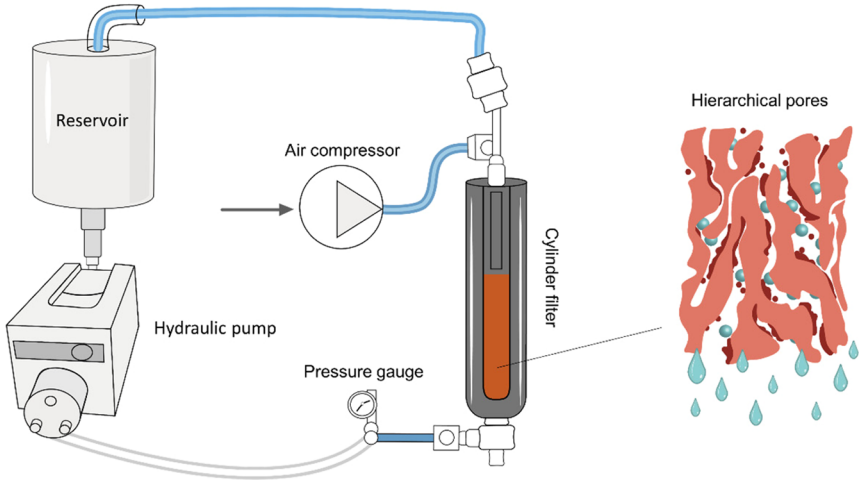

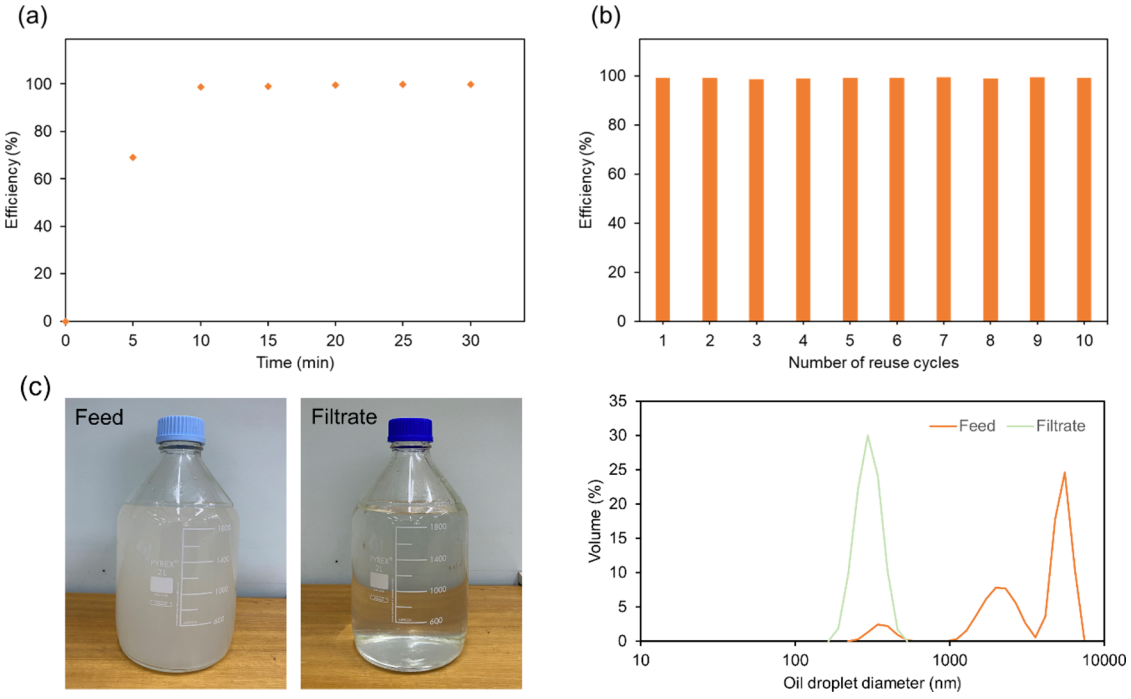

Figure 5. (a) O/W separation efficiency of MF-HCP-PDMS as a function of time. (b) Reuse of MF-HCP-PDMS. (c) Illustration of one cycle of separation before and after, as well as the size distribution of emulsions in the feed (average 3.6 μm) and filtrate (average 0.35 μm).

https://doi.org/10.1021/acsami.1c11302
ACS Appl. Mater. Interfaces 2021, 13, 39925−39933

of MF-HCP and MF-HCP-PDMS-1 was examined by five adsorption/desorption cycles using a model oil by centrifugation (Figure 4). The use of centrifugation instead of mechanical compression allows for the efficient removal of the sorbates from the adsorbents. More importantly, this experiment indicates that the adsorption of oils not only exists among the macropores of the sponge but also the micropores of HCPs. This can be interpreted from the adsorption capacities and residual oils of MF-HCP and MF-HCP-PDMS-1 shown in Figure 4. Within expectations, there was a decrease in terms of overall adsorption capacity and barely any residual oil was observed by the last cycle in the case of MF-HCP due to the significant particle loss, which can be observed during the test. In contrast, MF-HCP-PDMS-1 showed a steady adsorption capacity and residual oil, indicating no particle loss during the adsorption/desorption cycles. These findings were in good agreement with the discussions before.

3.5. O/W Emulsion Separation. To evaluate the separation performance, Shell Tellus hydraulic fluids were used for generating O/W emulsions. The model oil composed of refined mineral oils with hydrocarbons from C10 to C34 and additives can easily form stable emulsions without the use of surfactants, which is desirable for the study. MF-HCP-PDMS (2 g) was loaded as the filter in a stainless-steel cylinder where 2 L of 1000 ppm O/W emulsion in a reservoir tank was pumped through for each experiment, as shown in Scheme 1. The HCP sorbent was repeatedly regenerated by the solvent washing method and reused after blow-drying. Hexane was employed as an inexpensive, relatively safe, and fast evaporation solvent that is pumped through a custom-built separator for a specified time to extract the adsorbed oils followed by decanting the mixture and drying the sorbent with an air compressor connected to the system. The constant flow rate was set at 50 mL/min due to the upper pressure limit of the system. As can be seen in Figure 5a, the separation efficiency as a function of separation time indicates that the efficiency reaches 98.8% (12 ppm left) after 10 min and the maximum efficiency of 99.8% (2 ppm left) within 30 min separation in the liter-scale experiment. Since the size of the sponge after loading into the cylinder is compressed to be one third of the original, which in turn makes the average pore size about 45 μm. Despite such a large pore size compared to micro-nano emulsions, the sorbent filter can still effectively separate the oil droplets above the average diameter of 350 nm (Figure 5c). This can be attributed to the adsorption of hierarchical pores existing in this unique superhydrophobic sponge (Scheme 1). The addition of HCPs accelerates breaking of the emulsions and diffusion of hydrocarbons into the sorbent. Given the particular discharge standard established by local regulators during the oil spill response, the recovered water on a temporary storage device could be decanted if the total petroleum hydrocarbons is below a certain amount, for instance, 15 ppm, according to international law (MARPOL 73/78); therefore, the ultrahigh efficiency of MF-HCP-PDMS is far superior for decanting applications. Figure 5b shows the long-term robustness of MF-HCP-PDMS, and the performance is highly consistent over 10 cycles and remains the same after a total amount of 40 L of emulsions was tested.

4. CONCLUSIONS

By simply varying the reaction concentration and time of a hyper-cross-linked system, a novel HCP coating has been developed. This method introduces highly porous HCPs on a 3D porous matrix, which is reported for the first time. The existing relevant works involve column packing of porous polymers as solid phase extraction (SPE), fiber-based solid phase microextraction (SPME), where preformed porous polymers are fixed using silicone adhesives, and preparation of magnetic porous organic polymers, which are not versatile strategies for other applications.[36] We anticipate this method is potentially applicable for numerous desired surfaces with tunable loading, surface area, porosity, pore diameter, and surface chemistry for specific use. There are also alternative approaches using nonhalogenated reagents, which are possible without DCX used in this study.[20] The facile fabrication of the sorbent material requires inexpensive starting materials and mild operating conditions favorable for scale-up and therefore practical application in oil spill cleanup and wastewater treatment. The recyclability of MF-HCP indicated that the lifespan of such porous coating is limited. Therefore, the introduction of PDMS binders for robustness is necessary. This strategy guaranteed the long-lasting durability and optimized surface wettability without compromising the surface area of HCPs, resulting in ultrahigh efficiency for O/W emulsion separation and recovery. To further remove the oil droplets, for instance, below 100 nm, is also theoretically achievable by tuning the pore size of the substrate. We believe the HCP-decorated sponge has great potential for water treatment and meets the stringent discharge standards of effluents containing petroleum hydrocarbons into the marine environment.

■ ASSOCIATED CONTENT

Supporting Information

The Supporting Information is available free of charge at https://pubs.acs.org/doi/10.1021/acsami.1c11302.

SEM images of polydisperse HCPs synthesized from batch; photographs of various reaction concentrations and resulting coatings; SEM images and elemental analysis of HCP coating upon the surface of the sponge; FTIR characterizations of the pristine sponge, MF-HCP, and MF-HCP-PDMS, as well as $HCP_{surface}$ and HCP_{batch}; oil contact angle and time-lapse images of oil adsorption of MF-HCP-PDMS and MF-PDMS; adsorption capacities of MF-HCP-PDMS-2 toward different solvents and oils; and table of total surface area, pore volume, and pore size of modified substrates (PDF)

"Silver Mirror" effect (Movie S1) (MP4)

Adsorption of light oils (Movie S2) (MP4)

Adsorption of heavy oils (Movie S3) (MP4)

■ AUTHOR INFORMATION

Corresponding Authors

Wendy Tian − *Manufacturing, Commonwealth Scientific Industrial Research Organisation (CSIRO), Clayton, Victoria 3168, Australia*; Email: wendy.tian@csiro.au

Colin D. Wood − *Energy Business Unit, Commonwealth Scientific Industrial Research Organisation (CSIRO), Kensington, Western Australia 6151, Australia*; orcid.org/0000-0001-6160-0112; Email: colin.wood@csiro.au

Author

Qi Sheng − *Energy Business Unit, Commonwealth Scientific Industrial Research Organisation (CSIRO), Kensington,*

Western Australia 6151, Australia; orcid.org/0000-0001-6351-7099

Complete contact information is available at: https://pubs.acs.org/10.1021/acsami.1c11302

Notes

The authors declare no competing financial interest.

■ ACKNOWLEDGMENTS

We thank Malisja de Vries and Mark Greaves from Materials and Characterisation in CSIRO Clayton for their assistance in SEM and Kristina Konstas for the BET measurements. We also thank Nick Rigopoulos for providing access to the contact angle measurement instrument and George Maurdev for the Zetasizer. The research work was supported by department of Fisheries and Oceans Canada (grant no. MECTS-3955465).

■ REFERENCES

(1) Chen, C.; Weng, D.; Mahmood, A.; Chen, S.; Wang, J. Separation Mechanism and Construction of Surfaces with Special Wettability for Oil/Water Separation. *ACS Appl. Mater. Interfaces* **2019**, *11*, 11006−11027.

(2) Xue, Z.; Cao, Y.; Liu, N.; Feng, L.; Jiang, L. Special wettable materials for oil/water separation. *J. Mater. Chem. A* **2014**, *2*, 2445−2460.

(3) Zhang, W.; Liu, N.; Cao, Y.; Lin, X.; Liu, Y.; Feng, L. Superwetting Porous Materials for Wastewater Treatment: from Immiscible Oil/Water Mixture to Emulsion Separation. *Adv. Mater. Interfaces* **2017**, *4*, 1600029.

(4) Guo, H.; Yang, J.; Xu, T.; Zhao, W.; Zhang, J.; Zhu, Y.; Wen, C.; Li, Q.; Sui, X.; Zhang, L. A Robust Cotton Textile-Based Material for High-Flux Oil−Water Separation. *ACS Appl. Mater. Interfaces* **2019**, *11*, 13704−13713.

(5) Li, X.; Cao, M.; Shan, H.; Handan Tezel, F.; Li, B. Facile and Scalable Fabrication of Superhydrophobic and Superoleophilic PDMS-co-PMHS Coating on Porous Substrates for Highly Effective Oil/Water Separation. *Chem. Eng. J.* **2019**, *358*, 1101−1113.

(6) Jiang, B.; Chen, Z.; Dou, H.; Sun, Y.; Zhang, H.; Gong, Z. Q.; Zhang, L. Superhydrophilic and Underwater Superoleophobic Ti Foam with Fluorinated Hierarchical Flower-like TiO2 Nanostructures For Effective Oil-in-Water Emulsion Separation. *Appl. Surf. Sci.* **2018**, *456*, 114−123.

(7) Wang, C.-F.; Chen, L.-T. Preparation of Superwetting Porous Materials for Ultrafast Separation of Water-in-Oil Emulsions. *Langmuir* **2017**, *33*, 1969−1973.

(8) Zhang, W.; Liu, N.; Xu, L.; Qu, R.; Chen, Y.; Zhang, Q.; Liu, Y.; Wei, Y.; Feng, L. Polymer-Decorated Filter Material for Wastewater Treatment: In Situ Ultrafast Oil/Water Emulsion Separation and Azo Dye Adsorption. *Langmuir* **2018**, *34*, 13192−13202.

(9) Liu, M.; Tie, L.; Li, J.; Hou, Y.; Guo, Z. Underoil Superhydrophilic Surfaces: Water Adsorption in Metal−Organic Frameworks. *J. Mater. Chem. A* **2018**, *6*, 1692−1699.

(10) Singh, V.; Nguyen, T. P.; Sheng, Y.-J.; Tsao, H.-K. Stress-Driven Separation of Surfactant-Stabilized Emulsions and Gel Emulsions by Superhydrophobic/Superoleophilic Meshes. *J. Phys. Chem. C* **2018**, *122*, 24750−24759.

(11) Wang, C.-F.; Tsai, Y.-J.; Kuo, S.-W.; Lee, K.-J.; Hu, C.-C.; Lai, J.-Y. Toward Superhydrophobic/Superoleophilic Materials for Separation of Oil/Water Mixtures and Water-in-Oil Emulsions Using Phase Inversion Methods. *Coatings* **2018**, *8*, 396.

(12) Cao, Y.; Liu, N.; Zhang, W.; Feng, L.; Wei, Y. One-Step Coating Toward Multifunctional Applications: Oil/Water Mixtures and Emulsions Separation and Contaminants Adsorption. *ACS Appl. Mater. Interfaces* **2016**, *8*, 3333−3339.

(13) Wu, J.; Ding, Y.; Wang, J.; Li, T.; Lin, H.; Wang, J.; Liu, F. Facile Fabrication of Nanofiber-and Micro/Nanosphere-Coordinated PVDF Membrane with Ultrahigh Permeability of Viscous Water-in-Oil Emulsions. *J. Mater. Chem. A* **2018**, *6*, 7014−7020.

(14) Chen, T.; Duan, M.; Fang, S. Fabrication of Novel Superhydrophilic and Underwater Superoleophobic Hierarchically Structured Ceramic Membrane and its Separation Performance of Oily Wastewater. *Ceram. Int.* **2016**, *42*, 8604−8612.

(15) Peng, H.; Wu, J.; Wang, Y.; Wang, H.; Liu, Z.; Shi, Y.; Guo, X. A Facile Approach For Preparation of Underwater Superoleophobicity Cellulose/Chitosan Composite Aerogel For Oil/Water Separation. *Appl. Phys. A* **2016**, *122*, 516.

(16) Si, Y.; Fu, Q.; Wang, X.; Zhu, J.; Yu, J.; Sun, G.; Ding, B. Superelastic and Superhydrophobic Nanofiber-Assembled Cellular Aerogels for Effective Separation of Oil/Water Emulsions. *ACS Nano* **2015**, *9*, 3791−3799.

(17) Han, X.; Hu, J.; Chen, K.; Wang, P.; Zhang, G.; Gu, J.; Ding, C.; Zheng, X.; Cao, F. Self-assembly and Epitaxial Growth of Multifunctional Micro-Nano-Spheres for Effective Separation of Water-in-Oil Emulsions with Ultra-High Flux. *Chem. Eng. J.* **2018**, *352*, 530−538.

(18) Yang, X.; Tan, L.; Xia, L.; Wood, C. D.; Tan, B. Hierarchical Porous Polystyrene Monoliths from PolyHIPE. *Macromol. Rapid Commun.* **2015**, *36*, 1553−1558.

(19) Dawson, R.; Cooper, A. I.; Adams, D. J. Nanoporous organic polymer networks. *Prog. Polym. Sci.* **2012**, *37*, 530−563.

(20) Tan, L.; Tan, B. Hypercrosslinked porous polymer materials: design, synthesis, and applications. *Chem. Soc. Rev.* **2017**, *46*, 3322−3356.

(21) Liu, S.; Hu, Q.; Zheng, J.; Xie, L.; Wei, S.; Jiang, R.; Zhu, F.; Liu, Y.; Ouyang, G. Knitting aromatic polymers for efficient solid-phase microextraction of trace organic pollutants. *J. Chromatogr. A* **2016**, *1450*, 9−16.

(22) Pan, B.; Pan, B.; Zhang, W.; Lv, L.; Zhang, Q.; Zheng, S. Development of polymeric and polymer-based hybrid adsorbents for pollutants removal from waters. *Chem. Eng. J.* **2009**, *151*, 19−29.

(23) Feng, Y.; Yao, J. Design of Melamine Sponge-Based Three-Dimensional Porous Materials toward Applications. *Ind. Eng. Chem. Res.* **2018**, *57*, 7322−7330.

(24) Ruan, C.; Ai, K.; Li, X.; Lu, L. A Superhydrophobic Sponge with Excellent Absorbency and Flame Retardancy. *Angew. Chem., Int. Ed.* **2014**, *53*, 5556−5560.

(25) Gao, M.-L.; Zhao, S.-Y.; Chen, Z.-Y.; Liu, L.; Han, Z.-B. Superhydrophobic/Superoleophilic MOF Composites for Oil−Water Separation. *Inorg. Chem.* **2019**, *58*, 2261−2264.

(26) Han, N.; Zhang, Z.; Gao, H.; Qian, Y.; Tan, L.; Yang, C.; Zhang, H.; Cui, Z.; Li, W.; Zhang, X. Superhydrophobic Covalent Organic Frameworks Prepared via Pore Surface Modifications for Functional Coatings under Harsh Conditions. *ACS Appl. Mater. Interfaces* **2020**, *12*, 2926−2934.

(27) Jiang, Z.-R.; Ge, J.; Zhou, Y.-X.; Wang, Z. U.; Chen, D.; Yu, S.-H.; Jiang, H.-L. Coating sponge with a hydrophobic porous coordination polymer containing a low-energy CF3-decorated surface for continuous pumping recovery of an oil spill from water. *NPG Asia Mater.* **2016**, *8*, e253−e253.

(28) Sun, Q.; Aguila, B.; Perman, J. A.; Butts, T.; Xiao, F.-S.; Ma, S. Integrating Superwettability within Covalent Organic Frameworks for Functional Coating. *Chem* **2018**, *4*, 1726−1739.

(29) Xu, Z.; Wang, J.; Li, H.; Wang, Y. Coating sponge with multifunctional and porous metal-organic framework for oil spill remediation. *Chem. Eng. J.* **2019**, *370*, 1181−1187.

(30) Heale, F. L.; Einhorn, M.; Page, K.; Parkin, I. P.; Carmalt, C. J. Dual-scale TiO2 and SiO2 particles in combination with a fluoroalkylsilane and polydimethylsiloxane superhydrophobic/superoleophilic coating for efficient solvent−water separation. *RSC Adv.* **2019**, *9*, 20332−20340.

(31) Turco, A.; Primiceri, E.; Frigione, M.; Maruccio, G.; Malitesta, C. An innovative, fast and facile soft-template approach for the fabrication of porous PDMS for oil−water separation. *J. Mater. Chem. A* **2017**, *5*, 23785−23793.

(32) Yu, C.; Yu, C.; Cui, L.; Song, Z.; Zhao, X.; Ma, Y.; Jiang, L. Facile Preparation of the Porous PDMS Oil-Absorbent for Oil/Water Separation. *Adv. Mater. Interfaces* **2017**, *4*, No. 1600862.
(33) Moon, S.-Y.; Bae, J.-S.; Jeon, E.; Park, J.-W. Organic Sol−Gel Synthesis: Solution-Processable Microporous Organic Networks. *Angew. Chem., Int. Ed.* **2010**, *49*, 9504−9508.
(34) Yang, Y.; Tan, B.; Wood, C. D. Solution-processable hypercrosslinked polymers by low cost strategies: a promising platform for gas storage and separation. *J. Mater. Chem. A* **2016**, *4*, 15072−15080.
(35) Vakarelski, I. U.; Patankar, N. A.; Marston, J. O.; Chan, D. Y. C.; Thoroddsen, S. T. Stabilization of Leidenfrost vapour layer by textured superhydrophobic surfaces. *Nature* **2012**, *489*, 274−277.
(36) He, M.; Ou, X.; Wang, Y.; Chen, Z.; Li, D.; Chen, B.; Hu, B. Porous organic frameworks-based (micro)extraction. *J. Chromatogr. A* **2020**, *1609*, No. 460477.

https://doi.org/10.1021/acsami.1c11302
ACS Appl. Mater. Interfaces 2021, 13, 39925−39933